[67]R. E. Phillips and S. T. Thornton, Oak Ridge National Laboratory Report No. ORNL-4179, 1967 (unpublished).
[68]J. Orear, University of California Radiation Laboratory Report No. UCRL-8417, 1958 (unpublished);
A. McFarlane Mood, *Introduction to the Theory of Statistics* (McGraw-Hill Book Company, New York, 1950), p. 152.

PHYSICAL REVIEW C VOLUME 3, NUMBER 3 MARCH 1971

Proton Stripping Strengths for Levels of $^{11}C^{\dagger}$

J. R. Comfort,* H. T. Fortune,‡ J. V. Maher,§ and B. Zeidman
Argonne National Laboratory, Argonne, Illinois 60439
(Received 13 November 1970)

States of ^{11}C were studied with the $^{10}B(^3He, d)^{11}C$ reaction at a bombarding energy of 21 MeV. The data were found to favor the assignments $J^{\pi} = \frac{7}{2}^+$ and $\frac{5}{2}^+$ to the levels at 8.65 and 8.69 MeV, respectively. A distorted-wave analysis of the angular distributions for negative-parity states in ^{11}C yielded spectroscopic factors whose relative values agreed well with the predictions of Cohen and Kurath, even though the excited-state energies were found to be in better agreement with the predictions of the unified rotational model.

I. INTRODUCTION

The mirror nuclei ^{11}B and ^{11}C have been extensively studied and many of their properties are known.[1] Not so well known, however, are the single-particle strengths of the states as observed in the reactions $^{10}B(d, p)^{11}B$ and $^{10}B(^3He, d)^{11}C$. These are of considerable interest, since they may be compared directly with the predictions of the nuclear shell-model calculations of Cohen and Kurath[2,3] and Goldhammer *et al.*[4,5]

In previous work, the spectroscopic strengths for (d, p) reactions,[6,7] (d, n) reactions,[8] and $(^3He, d)$ reactions[9,10] on ^{10}B have generally been derived from analyses with plane-wave Born-approximation (PWBA) stripping codes. The absolute values of the strengths thus obtained are seldom accurate, and even the relative strengths are uncertain.

It has been shown[11,12] that distorted-wave Born approximation (DWBA) analyses are reasonably capable of fitting the angular distributions for single-particle transfer reactions on targets in the $1p$ shell and that the spectroscopic factors obtained are in reasonable agreement with shell-model calculations. However, for the $^{10}B(d, p)^{11}B$ reaction, such analyses have been carried out[11] only for transitions to the three strongest states below 7-MeV excitation. Other DWBA analyses were confined to the ground-state transition.[13,14] For the $^{10}B(^3He, d)^{11}C$ reaction, a DWBA analysis has been reported[15] only for the ground-state transition at bombarding energies less than 10 MeV.

The reaction $^{10}B(^3He, d)^{11}C$ was studied here at a bombarding energy of 21 MeV. Some of these data have been discussed in a previous report[16] in which $J^{\pi} = \frac{3}{2}^-$ was assigned to the 8.11-MeV state of ^{11}C. In the present study, we consider a DWBA analysis of all states below the proton breakup threshold at 8.693 MeV. Absolute spectroscopic factors have been extracted and they are compared with the predictions of shell-model calculations.[2-5] The angular distribution of a broad ($\Gamma \approx 200$ keV) level at 10.68 MeV is presented and fitted with a distorted-wave calculation. The ground-state transition from the $^{12}C(^3He, d)^{13}N$ reaction is also discussed.

II. EXPERIMENTAL PROCEDURE

The Argonne FN tandem accelerator produced a beam of ^3He ions with an energy of about 20.9 MeV. The ^3He beam was incident on self-supporting ^{12}C and ^{10}B targets placed in the center of an 18-in. remotely controlled scattering chamber.[17] The ^{12}C target was approximately 60 $\mu g/cm^2$ thick and the ^{10}B target, enriched to about 96% ^{10}B, was about 100 $\mu g/cm^2$ thick. Each was oriented with its normal at about 30° to the beam direction. The data revealed the presence of oxygen in both targets, and traces of ^{11}B, ^{12}C, and ^{28}Si in the ^{10}B target.

A vertical beam profile on the targets was established by two beam-defining slits whose dimensions were $\frac{1}{16} \times \frac{3}{16}$ in. and which were spaced about 12 in. apart, with the second slit placed about 8 in. before the target. The solid angle subtended by the detector was also defined by a rectangular collimator of the same dimensions placed about 4 in. from the target.

The detector telescope was composed of silicon surface-barrier derectors. The ΔE detector was 500 μ thick, which was sufficient to stop the elastically scattered ^3He particles, and the E detector

was 2000 μ thick. An anticoincidence detector, also 2000 μ thick, was placed after the ΔE and E detectors. A fourth silicon surface-barrier detector, of 500-μ depletion depth, was placed separately at 25° to the beam direction and was used as a monitor of the elastically scattered ^{3}He particles.

Pulses from the detector telescope were fed to a conventional pulse-multiplication particle-identification circuit. The data were stored in a 4096-channel analyzer operated in the 1024×4 mode. Signals for tritons, deuterons, and protons (with the high-energy events eliminated by the anticoincidence circuit) were stored in the fourth, third, and second memory quadrants, respectively. Signals for ^{3}He and ^{4}He particles (obtained from the ΔE detector only) were stored in the first quadrant. A resolution width of about 50 keV was achieved. After each run, the contents of the analyzer were dumped onto magnetic tape for later analysis.

Before the data were acquired, the accuracy of the scattering angle was measured by determining the crossover for the reactions ^{1}H(^{3}He, ^{3}He)^{1}H and ^{12}C(^{3}He, ^{3}He′)^{12}C(4.43 MeV). The angle was found to be correct to 0.1° at 15°.

Data for ^{3}He-induced reactions on ^{12}C were obtained at 14 angles between 8 and 90° in the laboratory system. A short repeat measurement at 15° was taken at the end of the experiment. The data from this spectrum could not substantiate a variation in target thickness of more than 5%.

Data from the ^{10}B target were also obtained at the same 14 angles between 8 and 90°. Spectra obtained at angles of 20 and 55° are shown in Fig. 1. Pile-up effects in the electronics resulted in very poor resolution for the data at 8 and 11°, and precluded the analysis of most of these data. In addition, the ground-state group for the (^{3}He, d) reaction was absent for angles less than 42° because of the discriminator settings of the electronics. Consequently, the discriminator settings were revised and, using shorter exposures, data were obtained for 27 angles between 8 and 85°. Four of these angles coincided with those of the previous long exposures. A comparison of the data for these four pairs of angles showed that there was no deterioration of the target during the course of the experiment.

III. DATA PROCESSING

A. Data Analysis

Much of the data analysis was carried out with the aid of the computer programs QPLOT and AUTOFIT.[18] The first program plotted the spectra, one above another, with the Q value of the reaction as the abscissa. It confirmed the identification of the states of ^{11}C and ^{13}N, and allowed contaminants in the ^{10}B and ^{12}C targets to be readily identified. The second program carried out a sophisticated least-squares analysis of the peaks in the spectra, utilizing a prescribed peak shape, to obtain the positions and areas of the peaks.

All the levels in ^{11}C below the proton separation energy of 8.693 MeV were analyzed in the spectra from the long bombardments. Because of the small yields, the analysis of the ^{11}C spectra from the shorter exposures was limited to seven states—the four well-separated levels below 5 MeV, the strong state at 6.48 MeV, and the two states of special interest[16] at 8.11 and 8.42 MeV. Particle groups from the reaction ^{16}O(^{3}He, d)^{17}F(0.50) ob-

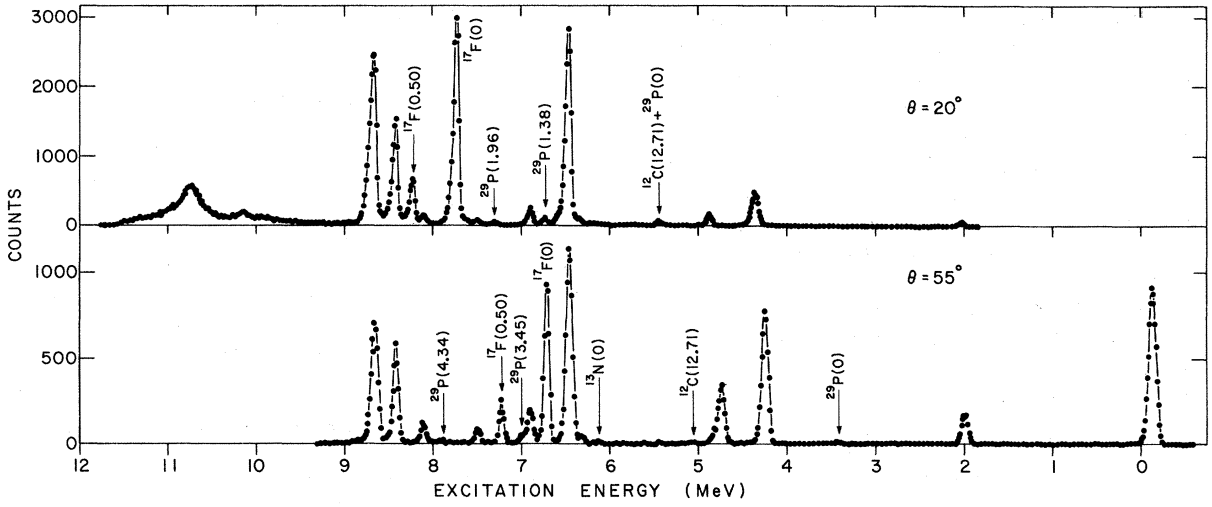

FIG. 1. Spectra of the ^{10}B(^{3}He, d)^{11}C reaction, obtained at angles of 20 and 55° for a beam energy of 21 MeV. The nonlinearity of the multichannel analyzer was represented only approximately by a polynomial. This causes a slight misplacement of some of the peaks on the excitation-energy scale.

scured the 8.11-MeV state between 24 and 28°.

Silicon on the ^{10}B target produced particle groups which were superimposed on some of the ^{11}C peaks at some angles. In most cases in which this occurred, the amount of contamination was so large or so uncertain that only upper limits could be established for the ^{11}C cross sections. However, for the 8.11-MeV state of ^{11}C at 36°, the contamination from the ^{28}Si(^{3}He, d)^{29}P(3.45) reaction was estimated and subtracted from the total yield. This estimate was obtained by observing the yield for this contaminant group at 42°, and extrapolating to 36° by using the measured angular distributions obtained[19] at a ^{3}He energy of 24.5 MeV. The amount subtracted was only one third of the total yield.

The levels at 8.652 and 8.694 MeV in ^{11}C were not entirely resolved in the present experiment. The program AUTOFIT was used to separate the two components, the positions and areas of the peaks being unconstrained. It was noticed that the separation of the peaks varied significantly with the angle, the average separation being 48 ± 4 keV. However, the peaks are known[1] to have a separation of 42 ± 6 keV. Using an average separation of 45 keV, the positions of the peaks were held fixed and AUTOFIT was requested to obtain their areas. Quite satisfactory results were obtained. Indeed, the angular distribution of the 8.65-MeV state was not noticeably modified, while that for the 8.69-MeV state showed slight changes.

The only identifiable levels above 9 MeV were those at 10.09 and 10.68 MeV. The 10.09-MeV level was too weak for an angular distribution to be extracted. The 10.68-MeV state was present in the spectra only for laboratory angles $\theta \leq 30°$. This state is broad ($\Gamma \approx 200$ keV) and rests on the three-body continuum. It also occurred near the low-energy cutoff of the spectra. Since the backgrounds could be only approximated, absolute cross sections could not be reliably obtained for this state. The angular distribution was, however, extracted in relative units by summing the counts above background over a prescribed energy interval. Care was taken that the same excitation-energy region was included in the sum at each angle.

The only state of ^{13}N of interest in this study was the ground state. It is the only bound state of ^{13}N. A more detailed study of the ^{12}C(^{3}He, d)^{13}N reaction was reported earlier.[12]

B. Absolute Cross Sections

The elastically scattered ^{3}He particles from the ^{10}B and ^{12}C targets were monitored during the course of the experimental measurements. The absolute-cross-section scale for ^{3}He-induced reactions on ^{12}C was established by comparing the yield for ^{3}He elastic scattering at $\theta_{lab} = 30°$ with the absolute cross section obtained from an earlier excitation function[20] measured at 30°. An excitation function had also been measured[20] at 45°. The normalization factor obtained by interpolating the present elastic scattering yields at 42 and 48° is consistent with the value obtained for the 30° cross sections. Also, the present data on the ^{12}C(^{3}He, d) reaction to the ^{13}N ground state were compared with the cross sections measured[21] at a beam energy of 21.64 MeV. These cross sections do not have a strong energy dependence.[21] The normalization factor thus obtained agreed with the previous value to within about 30%.

For the ^{10}B target, the absolute-cross-section scale was established by comparing the yield for ^{3}He elastic scattering with that from the ^{12}C target. The two elastic scattering angular distributions had identical shapes for $\theta_{c.m.} < 33°$ and the ratio of the yields was readily evaluated. This ratio was then corrected for the mass dependence of the elastic scattering cross sections by comparing the optical-model predictions of the scattering from ^{10}B and ^{12}C at very forward angles. The optical potentials were the same as those used in the distorted-wave analysis of the (^{3}He, d) reactions and are discussed in Sec. IV. Although the computed angular distributions did not have the same shape for angles larger than 15°, in contrast to the data, it is believed that this results from an improper optical potential and that a correction based on the cross sections at very forward angles is satisfactory. The absolute-cross-section scale thus obtained is thought to be accurate to about 30%.

The angular distributions for the levels of ^{11}C, expressed in the center-of-mass system, are shown in Figs. 2–5. The angular distribution for the ground state of ^{13}N is given in Fig. 6.

IV. DISTORTED-WAVE ANALYSIS

Distorted-wave calculations of the angular distributions have been carried out with the computer code DWUCK.[22] Such calculations for reactions in the $1p$ shell are known to be subject to many uncertainties, and close fits to data have seldom been achieved[11,12] for angles larger than 60°. Nevertheless, previous studies[11,12] have shown that it is possible to obtain useful spectroscopic information for such nuclei.

A. Parameter Selection

The real and imaginary terms of the optical-model potentials used in the present calculations are volume potentials with Woods-Saxon shapes. Coulomb potentials for uniform charge distributions are included. The parameters are listed in

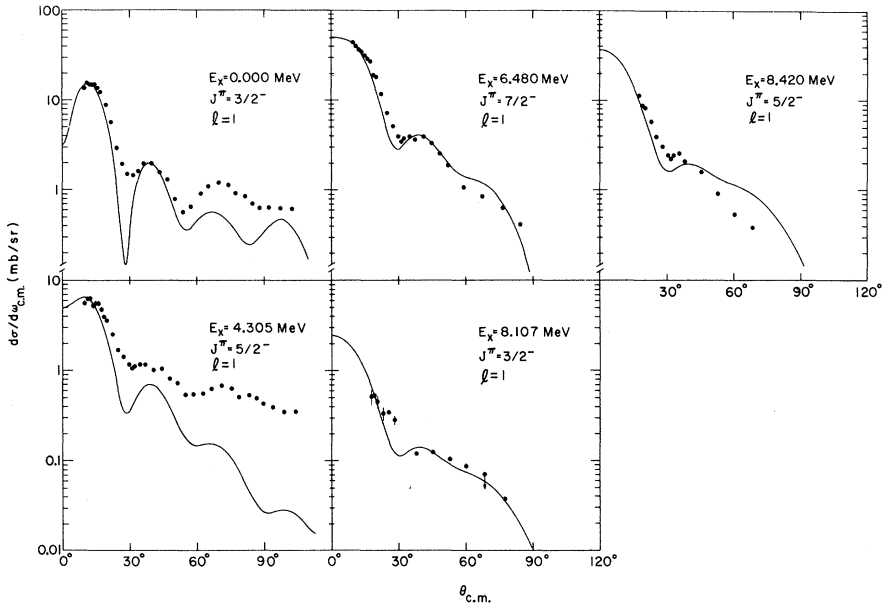

FIG. 2. Angular distributions for the negative-parity states of ^{11}C which exhibit stripping patterns. The curves are distorted-wave calculations.

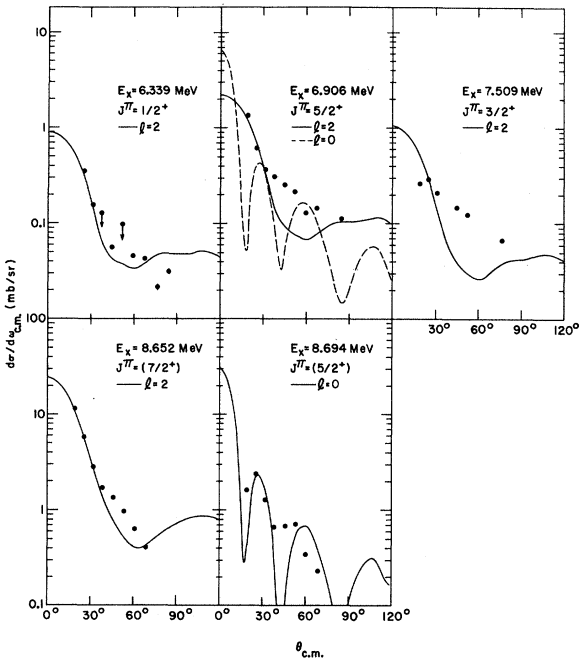

FIG. 3. Angular distributions for the bound positive-parity levels in ^{11}C. The curves are distorted-wave calculations. A downward-pointing arrow on a data point indicates that, at that angle, a known impurity group coincides with the ^{11}C group and has not been subtracted.

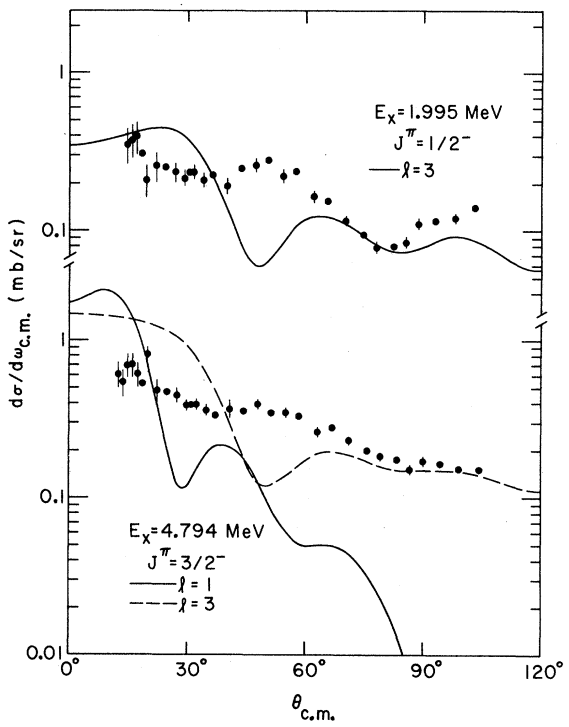

FIG. 4. Angular distributions for two negative-parity levels in ^{11}C which do not show characteristic stripping patterns. The curves are distorted-wave calculations.

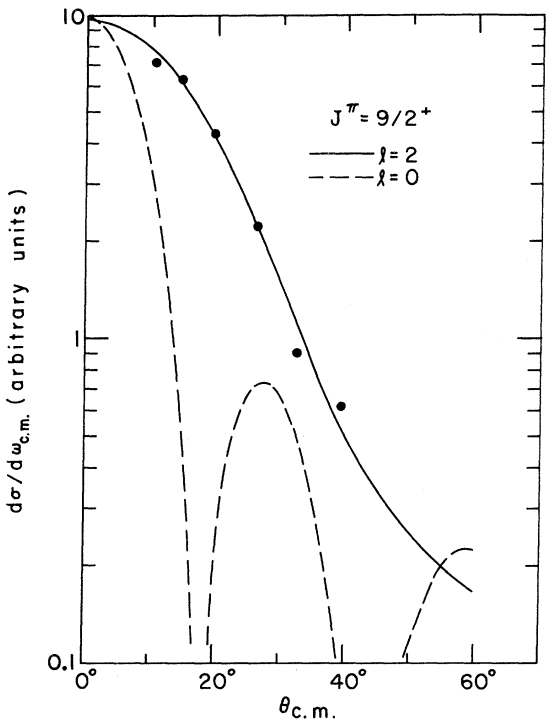

FIG. 5. Angular distribution for the unbound 10.68-MeV state of ^{11}C. The cross-sections scale is arbitrary and the curves are distorted-wave calculations.

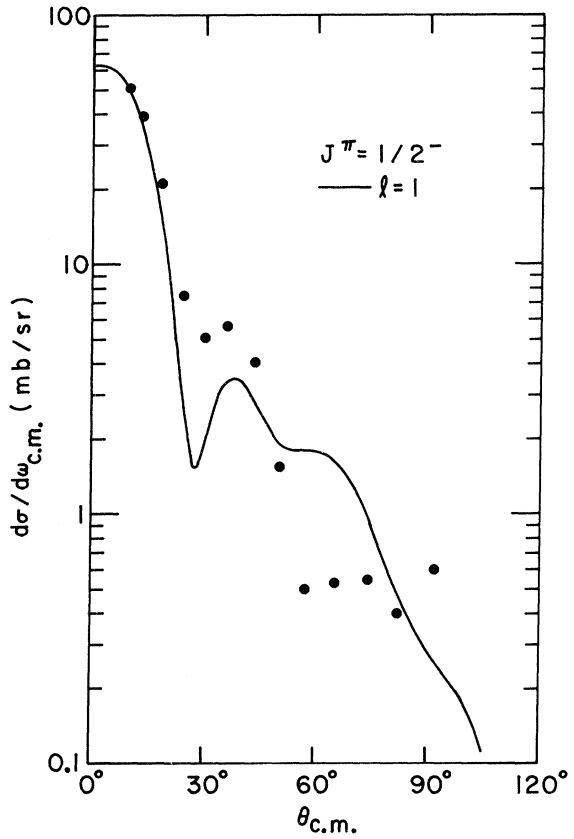

FIG. 6. Angular distribution for the ground state of ^{13}N. The curve results from a distorted-wave calculation.

Table I. Both the ^{3}He potential[23] and deuteron potential[12] were chosen to have "average" parameters. Even though such potentials will not in general fit specific elastic scattering data, they are expected to reproduce the systematic changes in the data as the target and beam energy are varied. Also, they are believed to be nearly free of resonance effects so that the computed angular distributions are relatively insensitive to small variations in the parameters.

A disturbing feature of the ^{3}He potential is the fact that it predicts quite different shapes for ^{3}He elastic scattering from ^{10}B and ^{12}C between 15 and 30°, although, as noted in Sec. III B, the data have similar shapes. Nevertheless, it is instructive to note that the optical potentials given in Table I have been found[24] to give good fits to the data for reactions on a variety of light nuclei.

The bound-state form factor was computed for a Woods-Saxon potential. The geometrical parameters (Table I) were taken from a previous study[12] of the ^{12}C(^{3}He, d)^{13}N reaction. The well depth was adjusted in order to reproduce the experimental binding energy of each state.

Spin-orbit terms were not included in the ^{3}He and deuteron potentials, since their effects were generally negligible. A spin-orbit term having the Thomas form and a strength $\lambda = 25$ was included in the bound-state potential, since this had some effect on the over-all magnitudes of the angular distributions.

Some consideration was given to the selection of the imaginary well depths, since these are poorly known. It was found that reasonable changes in $W(^3\text{He})$ and $W(d)$ did not noticeably affect the shapes of the angular distributions for angles less than 80 and 45°, respectively. The combination $W(^3\text{He}) = 15$ MeV and $W(d) = 14$ MeV produced the largest cross sections in the second and third maxima of the $l = 1$ angular distributions and was selected for the calculations. Even though there

TABLE I. Parameters for the bound-state and optical-model potentials used in the distorted-wave calculations. Well depths are in MeV and lengths in F.

Particle	V	r_0	a	W	r'	a'	r_C	V_{so}
^{3}He	177	1.138	0.7236	15	1.602	0.796	1.14	0
d	100	1.40	0.60	14	1.74	0.80	1.40	0
p	a	1.26	0.60				1.26	$\lambda = 25$

[a]Adjusted for each state to reproduce the experimental binding energies.

may be an energy dependence for $W(d)$, this dependence is not well known and its effects on the relative spectroscopic factors are not expected to be more than about 10% over the range of excitation energies considered in this experiment.

The effects of finite-range and nonlocality corrections were also investigated for the ground-state transition. The shape of the angular distribution was modified in the same manner as though both W parameters had been increased, and the theoretical cross section at the first maximum was increased by a factor of about 1.6. The extent to which finite-range and nonlocality corrections are required for the (^{3}He, d) reaction is not well known, and the final calculations were done without them.

B. Fitting the Data

The calculated angular distributions are shown with the data for ^{11}C in Figs. 2–5. The same parameters were also used in the calculation for the ^{13}N ground state and the curve is given in Fig. 6.

The $l=1$ curves in Fig. 2 generally provide a satisfactory fit to the data. Not only are the minima and maxima located in approximately the right places, but the Q dependence of the shapes appears to be satisfactorily reproduced. The worst fit occurs for the state at 4.305 MeV. These data most likely include contributions from $l=3$ stripping or from processes other than stripping.

Examples of angular distributions of these latter types are shown in Fig. 4. The $J^\pi=\frac{1}{2}^-$ assignment for the 1.995-MeV state precludes its population with an $l=1$ stripping pattern. An $l=3$ curve is shown for this state. The poor fit supports the belief that appreciable $1f_{7/2}$ strength should not be expected in ^{11}C. Although the selection rules would permit the population of the $J^\pi=\frac{3}{2}^-$ state at 4.794 MeV with $l=1$, it cannot be fitted with either $l=1$ or $l=3$. Indeed, its angular distribution is nearly identical to that for the 1.995-MeV state.

The positive-parity states (Fig. 3) were generally populated weakly by the (^{3}He, d) reaction. The states at 6.339 and 7.509 MeV cannot be populated with $l=0$ transitions, and the $l=2$ curves approximately represent the data. The 6.906-MeV state could be populated with both $l=0$ and $l=2$ transitions. The angular distribution clearly suggests that the $l=2$ shape is dominant.

The states at 8.652 and 8.694 MeV appear to be well fitted with $l=2$ and $l=0$ curves, respectively. Since the theoretical single-particle cross sections are larger for $l=2$ transitions, an $l=0$ component could be obscured for the 8.65-MeV state. The data points for the 8.69-MeV state are somewhat sensitive to the method used in resolving the doublet (Sec. III A), especially for the most forward angle. Nevertheless, the angular distribution always showed characteristics which differed from those of the 8.65-MeV state and substantiated the presence of a larger $l=0$ component. As shown, the data are fitted with a pure $l=0$ curve, although this probably overestimates the $2s_{1/2}$ strength.

The angular distribution for the 10.68-MeV state is well fitted with an $l=2$ curve (Fig. 5). An $l=0$ curve is shown for comparison even though the $J^\pi=\frac{9}{2}^+$ assignment[1] for this state precludes $l=0$ stripping. Since only the shape and not the absolute magnitude were required for this state, a fictitious binding energy of 0.01 MeV was used in the distorted-wave calculations for this state. However, the correct outgoing deuteron energy was used.

C. Spectroscopic Factors

The spectroscopic factors were obtained from the fits shown in Figs. 2–6 by use of the expression

$$\frac{d\sigma}{d\Omega}=4.42\,\frac{2J_f+1}{2J_i+1}\sum_l C^2S_l\,\frac{\sigma_{\mathrm{DWUCK}}(l)}{2j+1}, \tag{1}$$

where J_i, J_f, and j are the angular momenta of the ^{10}B ground state, the ^{11}C final state, and the transferred proton, respectively. All the final states have isospin $T=\frac{1}{2}$ and $C^2=1$. The normalization factor 4.42 is due to Bassel.[25] Table II gives the final results. Where possible, spectroscopic factors are given for both $1p_{3/2}$ and $1p_{1/2}$ transfers for $l=1$ transitions. The $l=0$, 2, and 3 transitions are assumed to involve transfers of $2s_{1/2}$, $1d_{5/2}$, and $1f_{7/2}$ particles, respectively.

The spectroscopic strengths are expected to obey the sum rule

$$\sum\frac{2J_f+1}{2J_i+1}C^2S=P_j, \tag{2}$$

where P_j is the number of proton holes in the single-particle orbit j in the target nucleus. In the present case, the sum of strengths for all $l=1$ transitions should be 3, regardless of how the protons are distributed among the $p_{3/2}$ and $p_{1/2}$ orbits, provided that no $1p$ particles in the target are excited to the s-d shell. Only the five states identified in Fig. 2 have sizeable $l=1$ strengths, and the sum of their weighted spectroscopic factors is 4.7–5.0, depending on the relative amounts of $p_{3/2}$ and $p_{1/2}$ components. The ratio to the sum-rule limit is about 1.6 and would correspond exactly to the factor that would be introduced by finite-range and nonlocality effects.

The spectroscopic factor of 1.13 for the ground state of ^{13}N agrees well with the value obtained[12] at lower bombarding energies and with different optical-model parameters. While the absolute values of all the spectroscopic factors may not be

TABLE II. Summary of the experimental results for l values and spectroscopic factors. The spectroscopic factors have not been renormalized to the sum rule nor have finite-range and nonlocality corrections been included.

E_x (MeV)	J^π	l	j	S
		^{11}C		
0.000	$\frac{3}{2}^-$	1	$\frac{3}{2}$	2.26
1.995	$\frac{1}{2}^-$	(3)	$(\frac{7}{2})$	<0.83
4.305	$\frac{5}{2}^-$	1	$\frac{3}{2}$	0.35
			or $\frac{1}{2}$	0.40
4.794	$\frac{3}{2}^-$	(1)	$(\frac{3}{2})$	<0.16
		(3)	$(\frac{7}{2})$	<0.73
6.339	$\frac{1}{2}^+$	2	$\frac{5}{2}$	0.16
6.480	$\frac{7}{2}^-$	1	$\frac{3}{2}$	1.52
			or $\frac{1}{2}$	1.65
6.906	$\frac{5}{2}^+$	2	$\frac{5}{2}$	0.12
		or 0	$\frac{1}{2}$	<0.09
7.509	$\frac{3}{2}^+$	2	$\frac{5}{2}$	0.08
8.107	$\frac{3}{2}^-$	1	$\frac{3}{2}$	0.14
8.420	$\frac{5}{2}^-$	1	$\frac{3}{2}$	1.51
			or $\frac{1}{2}$	1.65
8.652	$(\frac{7}{2})^+$	2	$\frac{5}{2}$	0.85
		or 0	$\frac{1}{2}$	<0.70
8.694	$(\frac{5}{2})^+$	0	$\frac{1}{2}$	<1.6
		^{13}N		
0.000	$\frac{1}{2}^-$	1	$\frac{1}{2}$	1.13

correct, it appears that the relative values do not depend significantly on the experimental conditions or on the distorted-wave analysis and should therefore contain useful information.

V. DISCUSSION

A. Doublet at 8.6 MeV

The levels at 8.65 and 8.69 MeV are excellent candidates for the analogs of the levels at 9.19 and 9.27 MeV in the mirror nucleus ^{11}B and would therefore have $J^\pi = \frac{7}{2}^+$ and $\frac{5}{2}^+$. However, the relative order of these assignments in ^{11}C is not known. Whether or not the levels cross when a neutron is changed into a proton, it is clear that the 9.27-MeV state moves down relative to the 9.19-MeV state.

Coulomb-energy calculations show that, relative to a p state at a similar binding energy, an s state moves downward and a d state moves upward when a neutron is changed into a proton. Therefore, the 9.27-MeV state must have more s strength or less d strength, or both, than the 9.19-MeV state. Hinds and Middleton[7] observed nearly equal $l=0$ strengths to these two levels in the ^{10}B$(d,p)^{11}$B reaction, and their data are consistent with more d strength in the 9.19-MeV state, as expected.

If the pairs of states in ^{11}B and ^{11}C are mirror levels, their spectroscopic strengths in single-particle transfer transfer reactions on ^{10}B, should be very similar. As discussed in Sec. IV B above, the data show that in ^{11}C the lower state contains more $l=2$ strength than does the upper state. The situation for $l=0$ is less clear. The $l=0$ strengths in the two states *could* be comparable, but it appears that the upper level contains more $l=0$ strength than does the lower state. This is entirely in accord with the strengths in ^{11}B and indicates that the levels have not crossed. Hence, the levels at 8.65 and 8.69 MeV in ^{11}C may be assigned as having $J^\pi = \frac{7}{2}^+$ and $\frac{5}{2}^+$, respectively.

B. Nuclear Models

Theoretical spectroscopic factors have been calculated by Cohen and Kurath[3] and by Varma and Goldhammer.[5] Both models evaluate the effective interactions in the $1p$ shell by fitting a number of well-identified levels for nuclei with masses $A=6$–16. Cohen and Kurath[2,3] incorporated only two-body interactions, whereas Goldhammer *et al.*[4,5] made corrections for three-body effects. The spectroscopic factors were calculated only for levels that could be reached by adding a $1p$ particle to the target nuclei.

The experimental and theoretical spectroscopic factors are compared in Table III. For the purpose of this comparison, the experimental spectroscopic factors have all been normalized to the theoretical value $S=1.09$ given by Cohen and Kurath for the ^{11}C ground state. The renormalization factor (about 2.1) is larger than that suggested by the sum-rule considerations or the finite-range and nonlocality corrections, but it simplifies the comparison of the relative values. The same value is also obtained from the ratio of experimental to theoretical[3] spectroscopic factors for the ^{13}N ground state. The experimental values are evaluated as though they arose entirely from $p_{3/2}$ transfers, or, if allowed, entirely from $p_{1/2}$ transfers. Cohen and Kurath[3] list separate components for $p_{3/2}$ and $p_{1/2}$ transfers, but Varma and Goldhammer[5] give only the sum.

The relative experimental values in Table III agree remarkably well with the values of Cohen and Kurath.[3] The agreement with the values of

TABLE III. Comparison of the (normalized) experimental relative spectroscopic factors for $l=1$ transitions with the predictions of Cohen and Kurath and of Goldhammer *et al.* The experimental spectroscopic factors have been normalized to a value of $S=1.09$ for the ground state.

		Relative spectroscopic factors					
		Expt. (norm.)		Cohen & Kurath [a]			
(MeV)	J^π	$p_{3/2}$	$p_{1/2}$	$p_{3/2}$	$p_{1/2}$	Sum	Goldhammer [b]
				^{11}C			
0.000	$\frac{3}{2}^-$	1.09		1.09		1.09	0.31
4.305	$\frac{5}{2}^-$	0.17	0.19	0.10	0.04	0.14	0.11
4.794	$\frac{3}{2}^-$	<0.08		0.005		0.005	0.01
6.480	$\frac{7}{2}^-$	0.73	0.79	0.05	0.82	0.87	0.57
8.107	$\frac{3}{2}^-$	0.07		0.21 (11.44 MeV) or 0.08 (13.36 MeV)		0.21 0.08	
8.420	$\frac{5}{2}^-$	0.73	0.79	0.17	0.65	0.82	0.79
				^{13}N			
0.000	$\frac{1}{2}^-$		0.55		0.61	0.61	0.56

[a] See Ref. 3.

[b] See Ref. 5.

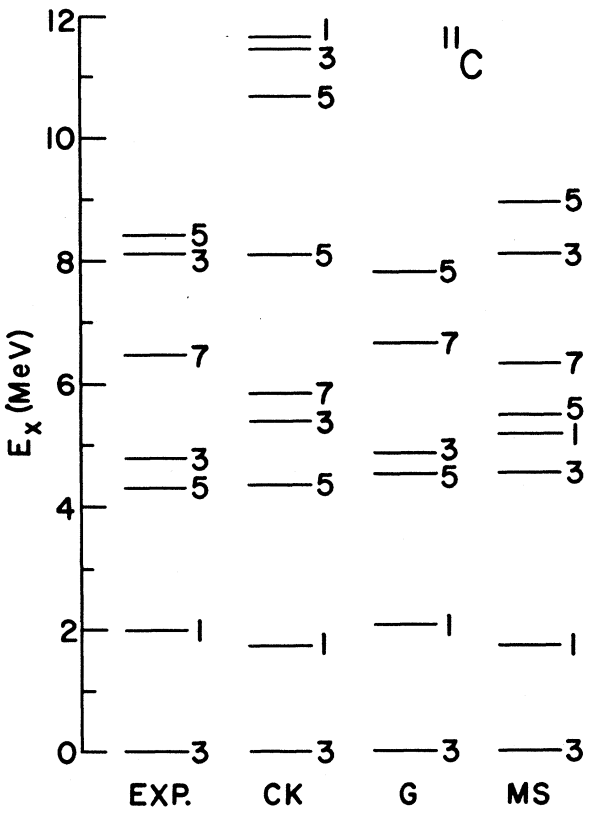

FIG. 7. The experimental (EXP.) and theoretical level schemes for odd-parity states of ^{11}C. The theoretical models are those of Cohen and Kurath (CK, Ref.2), Goldhammer *et al.* (G, Ref. 4), and Malik and Scholz (MS, Refs. 26, 27, and present paper). The number beside each level is $2J$, i.e., twice the spin of that level.

Varma and Goldhammer[5] is fair, the principal difference being the factor-of-3 discrepancy for the ground state of ^{11}C. Even though Goldhammer *et al.*[4,5] advise caution in interpreting the theoretical values too literally, this discrepancy is probably significant.

The third $J^\pi = \frac{3}{2}^-$ level in ^{11}C, observed experimentally at 8.11 MeV, is difficult to reconcile with theoretical predictions. Its relative spectroscopic factor agrees much better with the value Cohen and Kurath[3] computed for the fourth $\frac{3}{2}^-$ level (which they predict should be at 13.36 MeV) than for the third (predicted at 11.44 MeV). However, both theoretical levels lie much too high in energy, and neither one can be associated with the 8.11-MeV state simply on the basis of the spectroscopic factors.

In the weak-coupling model, it is possible to characterize the low-lying ($E_x<10$ MeV) negative-parity levels of ^{11}C as produced by coupling $p_{3/2}$ and $p_{1/2}$ holes to the 0^+ ground state and 2^+ first excited state of ^{12}C. This results in eight states: two with spin $\frac{1}{2}$, three with $\frac{3}{2}$, two with $\frac{5}{2}$, and one with $\frac{7}{2}$.

More sophisticated calculations also suggest the presence of this set of states in the low-lying spectrum of ^{11}C. The unified rotational model of Malik and Scholz,[26,27] which includes the Coriolis-coupling term, has been used to calculate the spectra of mass-11 nuclei. Calculations with a similar model have previously been reported[28] for nuclei in the $1p$ shell. The present calculations do not differ substantially from those of Ref. 28 except that here the deformation and moment-of-in-

ertia parameters were kept the same for all bands. Also, for the mass-11 nuclei, the best results in the present calculation were obtained with an oblate deformation $\beta = 0.30$, rather than with the large prolate deformation used in the previous calculations.[28]

The calculated level scheme for negative-parity states is shown in Fig. 7, along with the experimental level scheme and the schemes of the effective-interaction calculations.[2-5] In contrast to the latter models, the deformed model successfully reproduces the third $J^\pi = \frac{3}{2}^-$ state near 8 MeV. However, it also introduces a second $J^\pi = \frac{1}{2}^-$ level, not experimentally identified, near 6 MeV. The model of Cohen and Kurath places this level above 10 MeV.

Ground-state magnetic dipole moments have also been computed with the deformed model. The results are $-1.076\mu_N$ for ^{11}C and $+2.709\mu_N$ for ^{11}B. These are in excellent agreement with the experimental values[1] $(-)1.03\mu_N$ and $+2.688\mu_N$ for ^{11}C and ^{11}B, respectively.

The effective-interaction models were reported[2-5] to have unusual difficulties with the mass-11 nuclei, either with the level scheme or with some of the electromagnetic properties. The deformed model implicitly incorporates a slightly different type of effective interaction, although its shell-model representation is not transparent. The improvement exhibited by this model in some of the properties of ^{11}C and ^{11}B suggests that the shell models[2-5] may not include a sufficiently large basis and may not take proper account of the deformed core. Nevertheless, the excellent agreement between the relative spectroscopic factors from the ^{10}B(^{3}He, d)^{11}C reaction and those calculated by Cohen and Kurath[2,3] indicates that their model can well describe the principal characteristics of the negative-parity states of ^{11}C.

ACKNOWLEDGMENTS

We gratefully acknowledge several informative discussions with Dr. D. Kurath on the properties of the mass-11 system. We also especially thank Dr. B. Malik and Dr. W. Scholz for the use of their programs.

---

†Work performed under the auspices of the U. S. Atomic Energy Commission.

*Present address: Physics Department, Princeton University, Princeton, New Jersey 08540.

‡Present address: Department of Physics, University of Pennsylvania, Philadelphia, Pennsylvania 19104.

§Present address: Physics Department, University of Pittsburgh, Pittsburgh, Pennsylvania 15213.

[1]F. Ajzenberg-Selove and T. Lauritsen, Nucl. Phys. A114, 1 (1968).

[2]S. Cohen and D. Kurath, Nucl. Phys. 73, 1 (1965).

[3]S. Cohen and D. Kurath, Nucl. Phys. A101, 1 (1967).

[4]P. Goldhammer, J. R. Hill, and J. Nachamkin, Nucl. Phys. A106, 62 (1968).

[5]S. Varma and P. Goldhammer, Nucl. Phys. A125, 193 (1969).

[6]O. M. Bilaniuk and G. C. Hensel, Phys. Rev. 120, 211 (1960).

[7]S. Hinds and R. Middleton, Nucl. Phys. 38, 114 (1962).

[8]A. N. James, A. T. G. Ferguson, and C. M. P. Johnson, Nucl. Phys. 25, 282 (1961).

[9]P. D. Forsyth, F. deS. Barres, A. A. Joffe, I. J. Taylor, and S. Ramavataram, Proc. Phys. Soc. (London) A75, 291 (1960).

[10]S. Hinds and R. Middleton, Proc. Phys. Soc. (London) 78, 81 (1961).

[11]J. P. Schiffer, G. C. Morrison, R. H. Siemssen, and B. Zeidman, Phys. Rev. 164, 1274 (1967).

[12]H. T. Fortune, T. J. Gray, W. Trost, and N. R. Fletcher, Phys. Rev. 179, 1033 (1969).

[13]W. R. Smith and E. V. Ivash, Phys. Rev. 131, 304 (1963).

[14]H. W. Barz, R. Fülle, D. Netzband, R. Reif, K. Schlott, and J. Slotta, Nucl. Phys. 73, 473 (1965).

[15]J. R. Patterson, J. M. Poate, E. W. Titterton, and B. A. Robson, Proc. Phys. Soc. (London) 86, 1297 (1965).

[16]H. T. Fortune, J. R. Comfort, J. V. Maher, and B. Zeidman, Phys. Rev. C 2, 425 (1970).

[17]T. H. Braid and J. T. Heinrich, unpublished.

[18]J. R. Comfort, Argonne National Laboratory, Physics Division, Informal Report No. PHY-1970 B, 1970 (unpublished).

[19]H. Ejiri *et al.*, J. Phys. Soc. Japan 21, 2110 (1966).

[20]H. T. Fortune and N. Williams, unpublished.

[21]H. E. Wegner and W. S. Hall, Phys. Rev. 119, 1654 (1960).

[22]We are grateful to Professor Kunz for making his code DWUCK available to us.

[23]E. F. Gibson, B. W. Ridley, J. J. Kraushaar, M. E. Rickey, and R. H. Bassel, Phys. Rev. 155, 1194 (1967); H. T. Fortune, N. G. Puttaswamy, and J. L. Yntema, *ibid.* 185, 1546 (1969).

[24]J. V. Maher, H. T. Fortune, G. C. Morrison, and B. Zeidman, unpublished.

[25]R. H. Bassel, Phys. Rev. 149, 791 (1966).

[26]W. Scholz and F. B. Malik, Phys. Rev. 147, 836 (1966).

[27]F. B. Malik and W. Scholz, Phys. Rev. 150, 919 (1966).

[28]F. El-Batanoni and A. A. Kresnin, Nucl. Phys. 89, 577 (1966).